







Cite this: *Green Chem.*, 2020, **22**, 2077

## Biomimetic regioselective and high-yielding Cu(I)-catalyzed dimerization of sinapate esters in green solvent Cyrene™: towards sustainable antioxidant and anti-UV ingredients†

Matthieu M. Mention,  Amandine L. Flourat,  Cédric Peyrot  and Florent Allais \*

Naturally occurring sinapic acid and its esters are anti-UV and antiradical chemicals. This work aimed at designing an industrially relevant sustainable synthetic pathway allowing their selective  $\beta$ - $\beta'$  dimerization to enhance their properties with a view to use them in commercial applications such as functional additives for cosmetics, plastics and food/feed. A copper(I)-catalyzed procedure involving pyridine and O<sub>2</sub> from air was developed and greened up using the REACH-compliant bio-based solvent Cyrene™. Upon optimizing further through design of experiments, this sustainable synthetic process was successfully implemented to various sinapate esters and was validated on the multigram scale. Antiradical activities of the resulting  $\beta$ - $\beta'$  disinapate esters were benchmarked against commercial antioxidants, whereas their UV absorbance was compared to that of sinapoyl malate, a natural anti-UV compound found in plants and that of Octinoxate™, a widely used commercial sunscreen ingredient. Results showed that these dimers were better radical scavengers, and not only exhibited a better UV absorbance but also covered both UV-A and UV-B regions.

Received 10th January 2020,  
Accepted 16th February 2020

DOI: 10.1039/d0gc00122h

[rsc.li/greenchem](http://rsc.li/greenchem)

### Introduction

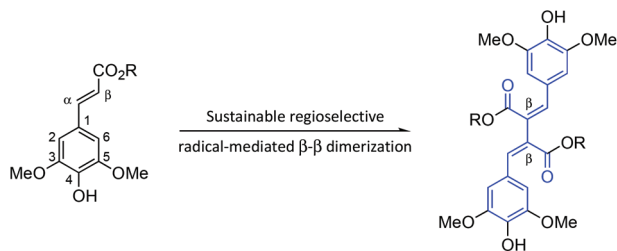
To decrease the imprint of humans on Earth, the demand for bio-based products with low ecological impact is rocketing. In this context, sinapic acid, a naturally occurring *p*-hydroxycinnamic acid mainly found in plants of the Brassicaceae family (*e.g.*, mustard, canola, and rapeseed),<sup>1</sup> seems to be a good candidate to develop new products, and more particularly antioxidants and anti-UV molecules that are able to replace the fossil-based ones currently criticized due to their toxicity. Indeed, several interesting properties have been reported for these molecules or their derivatives: antioxidant,<sup>1</sup> antimicrobial,<sup>2</sup> anti-inflammatory,<sup>3</sup> anticancer,<sup>4</sup> anxiolytic<sup>5</sup> and anti-UV.<sup>6–8</sup> It was shown that UV properties of sinapic ester derivatives result from (1) the conjugation between the C=C and C=O bonds (*i.e.*,  $\alpha,\beta$ -unsaturated ester) which allows electronic transition involving molecular orbitals throughout the entire sinapate part of the molecule and (2) the presence of a sterically hindered moiety in the  $\beta$  position that favors the *cis-trans* isomerization of sinapate esters upon UV exposure. Brassicaceae

species are extensively used in agriculture and generate a lot of by-products (*e.g.*, bran and oilcake) from which sinapic acid derivatives can be extracted.<sup>9–11</sup> It is noteworthy to mention that sinapic acid can also be efficiently synthesized by the Knoevenagel–Doebner condensation from syringaldehyde,<sup>12–16</sup> a *p*-hydroxybenzaldehyde obtained from the oxidation of hardwood lignins.<sup>17</sup> Given the properties cited above (*i.e.*, antiradical and anti-UV capacities) and their dependency on the degree of conjugation of the chemical structures, radical-mediated  $\beta$ - $\beta'$  dimerization of sinapic acid derivatives seemed an interesting approach to improve their antiradical and anti-UV properties, since such a dimerization further extends the conjugation and steric hindrance in the  $\beta$  position (Scheme 1).

However,  $\beta$ - $\beta'$  dimers of sinapic acid derivatives are difficult to synthesize in good yield and purity through radical–radical coupling as there are two radical species and thus two possible dimers –  $\beta$ -O-4' and  $\beta$ - $\beta'$  – that can oligomerize further. Moreover, in the case of sinapic acid, the  $\beta$ - $\beta'$  dimerization is usually followed by an intramolecular rearrangement leading to the formation of dilactone and the loss of conjugation (Scheme 2A).<sup>18</sup> To avoid the formation of such a dilactone, esters of sinapic acid can be used. On the basis of the above considerations, sinapate esters – more particularly ethyl sinapate – appeared as the most relevant substrates. In the literature, different pathways have been described for the synthesis

URD Agro-Biotechnologies Industrielles (ABI), CEBB, AgroParisTech, 51110 Pomacle, France. E-mail: [florent.allais@agroparistech.fr](mailto:florent.allais@agroparistech.fr)

† Electronic supplementary information (ESI) available. See DOI: 10.1039/d0gc00122h

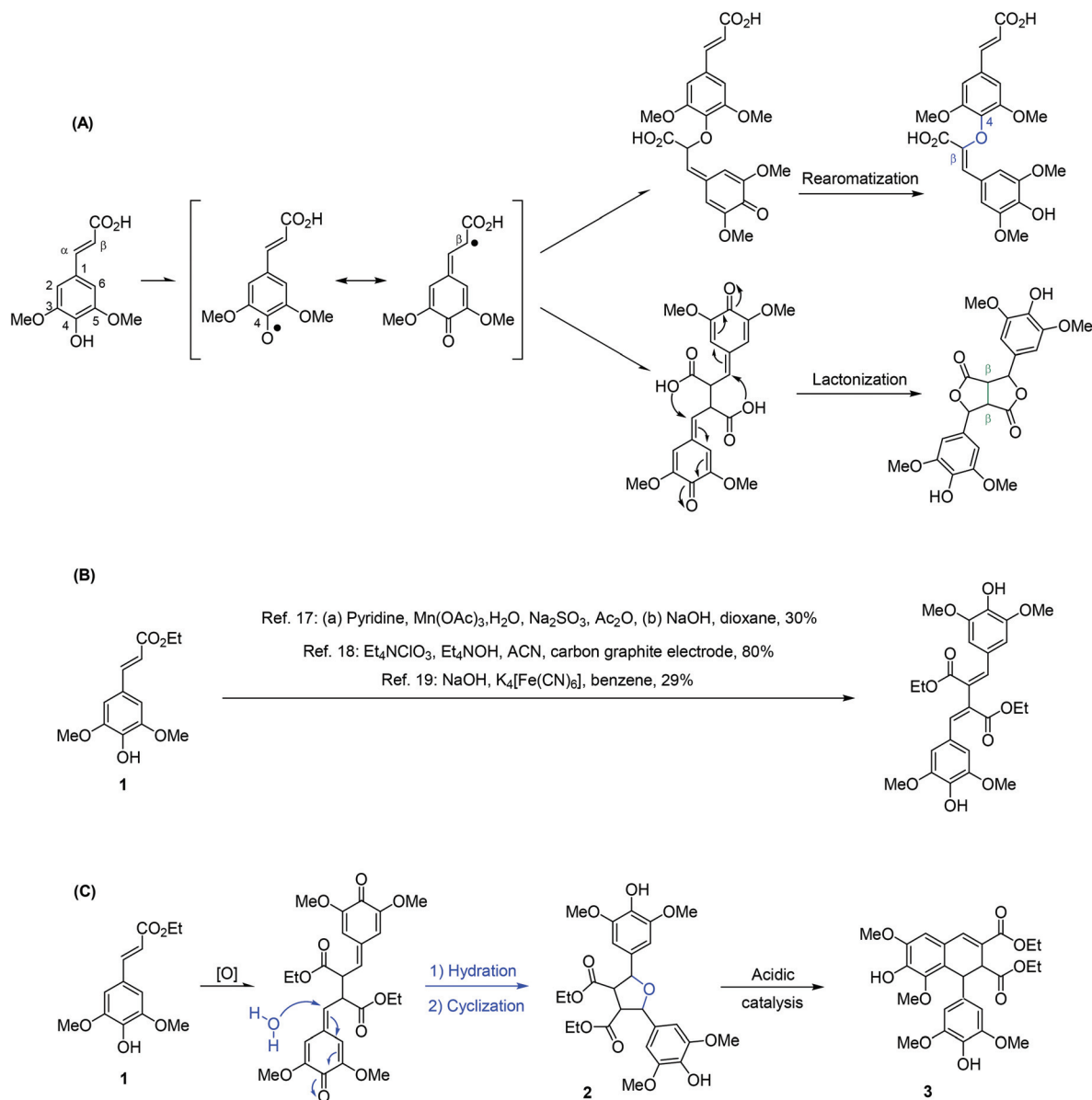


Extended conjugation within the entire molecule (aromatic & olefinic C=C as well as esters C=O):

- enhanced anti-UV activity?
- enhanced antiradical activity?

**Scheme 1** Will the extension of conjugation through the  $\beta$ - $\beta'$  dimerization of sinapate esters improve their anti-UV and antiradical properties?

of ethyl sinapate  $\beta$ - $\beta'$  dimers from ethyl sinapate (**1**): the first one relied on the  $\text{Mn}(\text{OAc})_2$ -mediated oxidation in the presence of  $\text{NaOH}$ ,<sup>19</sup> the second pathway involved an electrochemical oxidation with tetraethylammonium hydroxide and tetramethylammonium perchlorate,<sup>20</sup> and the third involved potassium ferrocyanide in benzene<sup>21</sup> (Scheme 2B). Although these procedures provide the desired target, not only do they use hazardous reagents, but also some of them have been proved ineffective on the multigram scale. It is also important to note that rearrangements can occur from the quinone methide intermediary with water, resulting in furan formation (**2**),<sup>22</sup> and a condensed linkage (**3**) under acidic conditions,<sup>23</sup> **2** and **3** being two compounds where the conjugation is significantly reduced (Scheme 2C). Designing a sustainable and scal-



**Scheme 2** (A)  $\beta$ - $O$ -4 and  $\beta$ - $\beta'$  dimers resulting from the oxidative dimerization of  $\beta$  sinapic acid, (B) previously reported syntheses of ethyl sinapate dimer and (C) rearrangement of the quinone methide intermediate.

able highly selective  $\beta$ - $\beta'$  dimerization synthetic process thus remains a challenge.

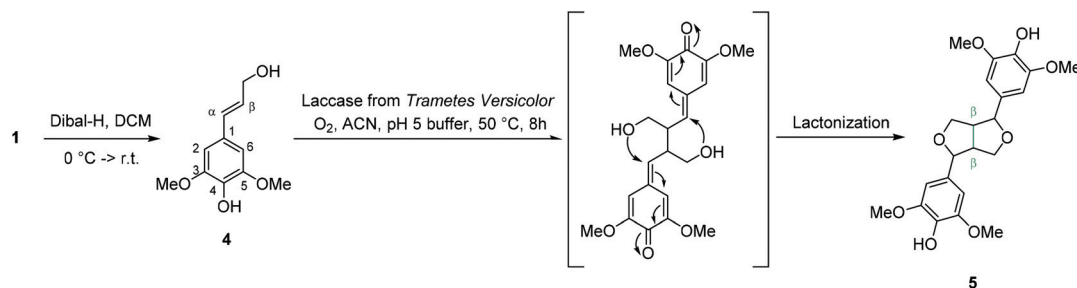
In this study, after having investigated different approaches, a highly selective copper(i)-catalyzed dimerization process in the REACH-compliant cellulose-based solvent Cyrene<sup>TM</sup> enabling the synthesis of  $\beta$ - $\beta'$  ethyl sinapate dimer on a multi-gram scale has been designed and optimized, and has been successfully implemented on various sinapate esters. To assess the importance of the extended conjugation and that of the ester moieties for their antiradical and anti-UV properties, the corresponding saturated  $\beta$ - $\beta'$  ethyl sinapate dimer and  $\beta$ - $\beta'$  sinapyl alcohol dimer were synthesized. Structure-activity relationships (SARs) were evaluated with regard to radical scavenging and UV absorbance activities. Antiradical properties of the  $\beta$ - $\beta'$  sinapate ester dimers were determined using the ABTS assay<sup>24</sup> and were compared to that of the commercial antioxidants (*i.e.*, BHT and BHA). For the anti-UV properties, sinapoyl malate, which has been described as the “sunscreen” of plants,<sup>6</sup> and Octinoxate<sup>TM</sup>, one of the most widespread anti-UV chemicals used in cosmetics, were used as references.

## Results and discussion

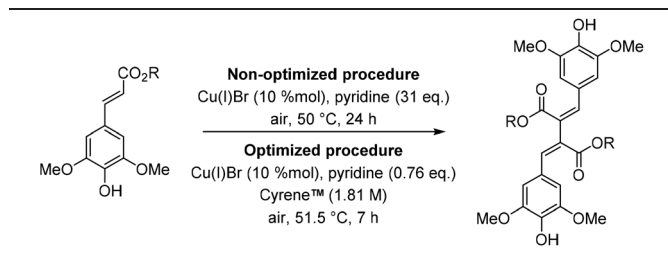
To investigate and optimize the  $\beta$ - $\beta'$  dimerization of sinapate esters, ethyl sinapate (**1**) was chosen as the model compound. In a previous work dedicated to the laccase-mediated dimerization of sinapyl alcohol (**4**) into syringaresinol (**5**) in 93% yield<sup>25</sup> (Scheme 3), we demonstrated that one can selectively favor the  $\beta$ - $\beta'$  dimerization over the  $\beta$ -O-4 one by finely tuning the reaction conditions (*i.e.*, slow addition of laccase from *Trametes versicolor* and a 4.9 pH buffer/acetonitrile). Encouraged by these promising results, this procedure was thus directly applied on ethyl sinapate. Unfortunately, UHPLC analysis (ESI, Fig. S1†) revealed that the reaction not only resulted in a mixture containing the desired  $\beta$ - $\beta'$  ethyl sinapate dimer **8**, but also the  $\beta$ -O-4' dimer (**6**), dimer 7 (obtained through the rearrangement of **8**), unreacted **1**, as well as soluble and insoluble oligomers, proving that the high selectivity observed with sinapyl alcohol was totally lost with ethyl sinapate. Further optimization was thus required. The presence of oligomers suggests a high affinity of the enzyme towards dimers **6**

and **8**, and to a larger extent towards the resulting oligomers. As an effort to prevent the contact between the enzyme and the targeted dimers, to limit the formation of (in)soluble oligomers, acetonitrile was replaced by ethyl acetate, thus providing a biphasic system where the dimers would be in the organic layer and the enzyme in the interphase. This modified procedure did prevent the formation of insoluble oligomers, but not that of soluble oligomers and dimers **6** and **7**. The formation of dimer **7** being promoted under acidic conditions,<sup>23</sup> the aqueous buffer was replaced by Milli-Q water. Under such conditions,  $\beta$ -O-4' and  $\beta$ - $\beta'$  dimers (**6** and **8**) were obtained along with traces of dimer **7** (ESI, Fig. S1†); however, soluble oligomers were recovered as major products and the selectivity of the dimerization remained in favor of the  $\beta$ -O-4' coupling. All our attempts that involved varying the reaction parameters (the co-solvent ratio, temperature, time, amount and the addition rate of the enzyme) proved unsuccessful. Laccase from *Trametes versicolor* seems to have too much affinity for our substrates, and it was decided to switch to horseradish peroxidase (HRP) type II and VI, these enzymes being known for their ability to promote the  $\beta$ - $\beta'$  coupling of *p*-hydroxycinnamic acid<sup>22,23,26,27</sup> and their lesser affinity for sinapic acid derivatives.<sup>28</sup> On the down side, as these enzymes exhibit low tolerance to organic solvents, the biphasic system could not be utilized. Once again, varying several conditions (temperature, type of HRP and the co-solvent ratio) only resulted in a decrease of oligomer formation, and no improvements were observed in terms of selectivity towards  $\beta$ - $\beta'$  coupling, and worse yet, dimer **7** formation was favoured.

As the use of enzymes proved quite unsuccessful, a different approach based on metal catalysis was investigated. Given the fact that laccase from *Trametes versicolor* seemed to have a high affinity toward ethyl sinapate and its dimer, we decided to mimic the active site of the enzyme composed of copper(i) and histidine,<sup>29</sup> by using copper(i) bromide, air (O<sub>2</sub>), and pyridine as a source of copper(i), an oxidizing agent, and a histidine surrogate, respectively. A first attempt using CuBr(i) (10 mol%) and pyridine (31 eq.) for 24 h at 50 °C provided  $\beta$ - $\beta'$  dimer in good yield (62%) and with high selectivity. Moreover, no trace of  $\beta$ -O-4' dimer or oligomers was observed. To widen the scope of this dimerization methodology, this procedure was performed on various sinapate esters (*i.e.*, heptyl sinapate, *tert*-butyl sinapate, 2-ethyl-hexyl sinapate, isopropyl sinapate



**Scheme 3** Highly regioselective laccase-catalysed synthesis of syringaresinol from ethyl sinapate.

**Table 1** Synthesis of sinapate  $\beta$ - $\beta'$  dimers (non-optimized and optimized procedures)

Compounds	R	Non-optimized procedure <sup>a</sup> (% yield)	Optimized procedure <sup>a</sup> (% yield)
8		62	89
9		64	90
10		55	88
11		58	89
12		58	91
13		42	87
14		42	88

<sup>a</sup> Isolated yields.

and guaiacol sinapate prepared by following the procedures described in the literature,<sup>30,31</sup> and sinapoyl *di*tert-butyl malate which was synthesized by following the method from Allais *et al.*<sup>32</sup>). Sinapate dimers were then obtained in average yields, ranging from 42% to 64% (Table 1).

### Optimization

To validate the proof of concept, and in the context of sustainable development, the next step was to green up the reaction by first reducing the quantity of pyridine used, by switching its role from being a solvent/ligand to only a ligand. To do so, some less toxic solvents were studied as an alternative to pyridine: ethyl acetate, ethanol, and Cyrene<sup>™</sup>, a REACH-compliant cellulose-derived polar aprotic solvent.<sup>33–35</sup> The screening of these solvents using the following conditions (Cu(I)Br (10 mol%), 1 equivalent of pyridine and ethyl sinapate at a concentration of 0.5 mol L<sup>-1</sup> in the different solvents) showed that Cyrene<sup>™</sup> was by far the most efficient (ESI, Fig. S2†). It is noteworthy to mention that DCM and DMSO, two other aprotic polar solvents, provided similar results. However, Cyrene<sup>™</sup> was chosen, as it fulfills all the criteria for a green reaction as it is a cellulose-derived sustainable solvent with a low vapor pressure (14.4 Pa at 25 °C) and low (eco)toxicity.<sup>33</sup> A

test without pyridine showed no conversion of ethyl sinapate, confirming that the Cu(I)-catalyst must be activated in the same way as the laccase active site.<sup>29</sup> Assays with DMAP (4-dimethylaminopyridine) and triethylamine in place of pyridine were performed to assess the type of amine needed for catalysis. Reaction using DMAP led to similar results than pyridine, while the use of triethylamine did not result in a good conversion of ethyl sinapate into its  $\beta$ - $\beta'$  dimer. Such results show that aromaticity of amine is needed to achieve good conversion and yield for the studied dimerization. Finally, in an effort to minimize the utilization of toxic compounds in the reaction further, pyridine was successfully reduced to 0.5 equivalent without affecting the  $\beta$ - $\beta'$  dimer yield (63%). Although this yield was acceptable, we decided to pursue the optimization of this reaction further through a Design of Experiments (DoE) and Response Surface Methodology (RSM). Before performing the DoE, a kinetic study was carried out to determine a relevant time scale. Monitoring of both the ethyl sinapate conversion and the yield of ethyl sinapate  $\beta$ - $\beta'$  dimer by HPLC showed that maximum yield was reached after 7 hours (69%), while the conversion continued to increase from 78% at 7 h to 98% at 24 h (Fig. 1). In view of these results, the duration was therefore fixed to 7 hours for the DoE. The DoE was elaborated to analyze the impact of four variables – Temperature (Temp), the Substrate/Catalyst ratio (S/C), the Amine/Catalyst ratio (A/C) and Concentration (Con) (Table 2) – on two responses, conversion of ethyl sinapate and yield of the desired product. For this purpose, a face-centered cubic design was chosen with triplicate at the central point and 27 experiments were performed

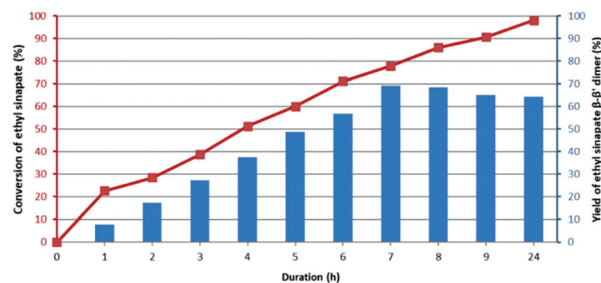


**Fig. 1** HPLC monitoring of the dimerization of ethyl sinapate: conversion of the starting material (red) and yield of ethyl sinapate  $\beta$ - $\beta'$  dimer (blue). [Zorbax Eclipse Plus C18 (2.1 mm  $\times$  50 mm  $\times$  1.8  $\mu$ m),  $\lambda$  = 320 nm, flow rate set at 0.6 mL min<sup>-1</sup>, oven temperature at 30 °C and gradient applied: H<sub>2</sub>O/CH<sub>3</sub>CN from 75/25 to 70/30 in 18 min].

**Table 2** Independent variables and levels used for the full factorial design

Variables	Levels		
	-1	0	1
Temp. (°C)	25	47.5	70
Ratio S/C	2	6	10
Ratio A/C	1	5.5	10
Con (mol L <sup>-1</sup> )	0.25	1.375	2.5



(ESI, the matrix in Table S1†). The reduction of the quantity of catalyst and amine, as well as the use of mild temperatures, were explored to green up the reaction further, besides improving the yield. For the same purpose, concentration of the reaction medium was increased to reduce both the environmental footprint and cost.

After the computational evaluation of the raw results, logit transformation ( $\log(Y)/(100 - Y)$ ) was applied for the yield, whereas no transformation was needed for the conversion. In addition, an outlier was found for the yield (ESI, entry N9 in Table S1†) and was excluded in the statistical analysis. Nevertheless, the validity of the model was still too low and presented a lack of fit in the *F*-tests performed using ANOVA, and that is why the points with the highest difference between the experimental value and the prediction of the model were duplicated (entries 28 to 32 in Table S1†) and included in the model to refine it. The quality of this refined model proved very good for both the yield ( $R^2 = 0.876$ ,  $Q^2 = 0.769$ , model validity = 0.912 and reproducibility = 0.850) and the conversion ( $R^2 = 0.936$ ,  $Q^2 = 0.901$ , model validity = 0.639 and reproducibility = 0.933) (ESI, Fig. S3†). Moreover, the analysis of the variance (ESI, Tables S2 and S3†) confirmed that the significance of the model was achieved ( $p < 0.05$ ); moreover, the lack of fit ( $p > 0.05$ ) showed a statistical significance of both models and a similar magnitude of replicate errors (no lack of fit). Sphericity of the design was assessed with condition numbers of 6.054 and 6.184 ( $< 8$ ) for the yield and the conversion, respectively.

Scaled and centered coefficients of the model (Fig. 2A and B) allowed determining the influence of each parameter, their square terms and also the quadratic effect. On both responses, the independent variables (*i.e.*, temperature, ratio S/C, ratio A/C and concentration) had a positive impact, the concentration (Con) being the most influential. Nevertheless, the significant square terms ( $\text{Temp}^2$ ,  $(\text{A/C})^2$  and  $\text{Con}^2$ ), all negatives, lowered the direct impact of the independent variables, leading to a decrease in the yield and the conversion for a variation too important from the central point. Once again, the most influential parameter was the square of the concentration ( $\text{Con}^2$ ). The interaction between the variables was evaluated with the quadratic terms. For the yield, the quadratic terms with positive contributions were the interaction between temperature and the amine/catalyst ratio ( $\text{Temp} \cdot \text{A/C}$ ) and the interaction between catalyst/substrate and amine/catalyst ratios ( $\text{S/C} \cdot \text{A/C}$ ). On the other hand, the  $\text{S/C} \cdot \text{Con}$  and  $\text{A/C} \cdot \text{Con}$  ratios had a negative impact. For the conversion of ethyl sinapate, the temperature was mainly involved, negatively with S/C and positively with A/C and Con. Finally, the quadratic term  $\text{S/C} \cdot \text{Con}$  impacted the conversion positively.

Direct visualization of the results obtained through the DoE was facilitated by using Response Surface Methodology (RSM), where optimal responses are represented by the red areas (Fig. 2). Clearly, high conversion of ethyl sinapate can be achieved under a large set of conditions (Fig. 2C). However, in order to maximize the yield, temperature had to be carefully adjusted (40–55 °C) in a restricted range of concentration

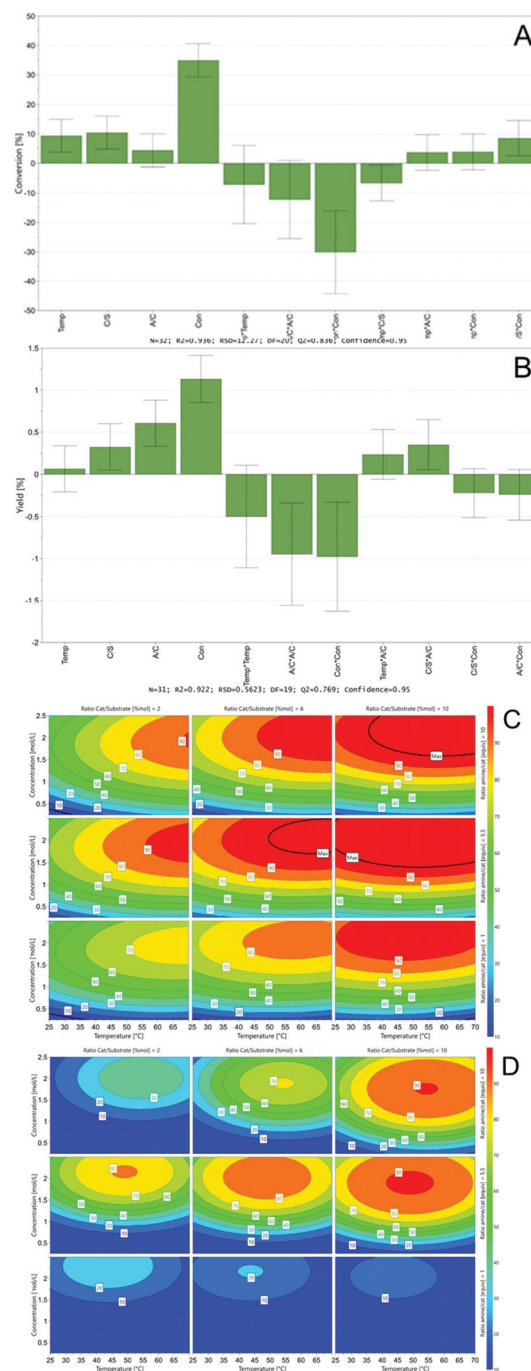


Fig. 2 Scaled and centered coefficients of the quadratic model for the conversion (A) and the yield (B) and the response surface for the conversion (C) and the yield (D) for the  $\beta$ - $\beta'$  dimerization of ethyl sinapate.

(1.5–2.0 mol L<sup>-1</sup>) with the highest amount of catalyst. In addition, an intermediate ratio of amine/catalyst enlarged the surface to lead to this high yield (Fig. 2D). Finally, to be able to predict the outcome of future experiments, equations of the model (eqn (1)) are expressed uncoded below in order to allow the direct numerical application, where *Y*<sub>1</sub> and *Y*<sub>2</sub> were the yield and the conversion, respectively.

Equations of the model:

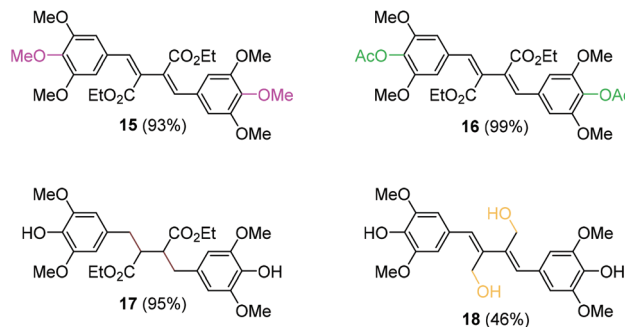
$$\begin{aligned} \text{Log}(Y1/(100 - Y1)) = & -6.9034 + 0.0840(\text{Temp}) + 0.0420(\text{S/C}) \\ & + 0.4879(\text{A/C}) + 3.6926(\text{Con}) - 0.0010(\text{Temp})^2 - 0.0469(\text{A/C})^2 \\ & - 0.7730(\text{Con})^2 + 0.0023(\text{Temp} \times \text{A/C}) + 0.0195(\text{S/C} \times \text{A/C}) \\ & - 0.0495(\text{S/C} \times \text{Con}) - 0.0478(\text{A/C} \times \text{Con}), \\ Y2 = & -75.7650 + 1.7907(\text{Temp}) + 3.5114(\text{S/C}) + 5.8929(\text{A/C}) \\ & + 77.7829(\text{Con}) - 0.0142(\text{Temp})^2 - 0.6055(\text{A/C})^2 \\ & - 23.8050(\text{Con})^2 - 0.0740(\text{Temp} \times \text{S/C}) + 0.0369(\text{Temp} \times \text{A/S}) \\ & + 0.1547(\text{Temp} \times \text{Con}) + 1.9015(\text{S/C} \times \text{Con}). \end{aligned} \quad (1)$$

To assess the predictability of the model, external validation was performed in duplicate using the optimal conditions predicted by the model (Table 3). In both cases, a total conversion was achieved, and the yields were 88% and 89%, respectively, a little lower than the prediction, but still within the 83.7–98.1% range achievable with this set of conditions, thus validating the model. To summarize, compared to the initial procedure, optimization by RSM allowed a significant improvement of the  $\beta$ - $\beta'$  dimerization of ethyl sinapate, with a yield increasing from 63% to 89%. Although we were not able to reduce the copper bromide amount without affecting the yield, the quantity of pyridine was reduced 41-fold, the reaction medium was concentrated up to 1.81 mol L<sup>-1</sup>, which represented a 3.6-fold diminution of the total volume of Cyrene™ and the duration was reduced from 24 to 7 hours (Table 3).

This optimized procedure was then successfully applied to the sinapate esters previously described (yields ranging from 87% to 91%) and was validated on the multigram scale (Table 1). It is noteworthy to mention that, for the optimized conditions, a simple extraction with ethyl acetate/1M aqueous HCl allowed the recovery of  $\beta$ - $\beta'$  dimers, while a purification using silica gel chromatography was needed for the non-optimized conditions. With the library of  $\beta$ - $\beta'$  sinapate ester dimers in hand, we then proceeded to the investigation of their antiradical and anti-UV properties. To establish SARs and determine the impact of the conjugation/unsaturations (*i.e.*, C=C), the esters and the phenol moieties, on the anti-UV and antiradical properties,  $\beta$ - $\beta'$  ethyl sinapate dimer (**8**) was (i) methylated (**15**), (ii) acetylated (**16**), (iii) reduced *via* palladium-catalyzed hydrogenation to provide its saturated counterpart (**17**), and (iv) reacted with DIBAL-H to give the corresponding dialcohol (**18**) (Scheme 4).

**Table 3** Optimal conditions predicted by the model and the comparison between initial and optimized  $\beta$ - $\beta'$  dimerization of ethyl sinapate

Conditions	Temp (°C)	S/C	A/C	Con (mol L <sup>-1</sup> )	t (h)	Conv. (%)	Yield (%)
Initial	50	10	310	0.5	24	99	62
Predicted	51.5	10	7.6	1.81	7	100	84–98
Optimized	51.5	10	7.6	1.81	7	99	89



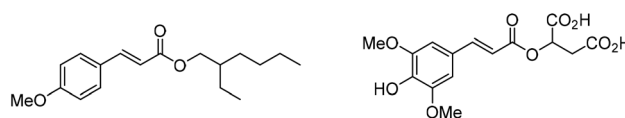
**Scheme 4** Dimers synthesized for SARs.

### Anti-UV properties

To assess the potential of our molecules as anti-UV compounds, Octinoxate™ (ethylhexyl methoxycinnamate) – a commercial anti-UV-B ingredient widely used in sunscreens and cosmetics – and sinapoyl malate – a naturally occurring anti-UV compound in plants<sup>6</sup> – have been used as benchmarks (Scheme 5).

As shown in Fig. 4, the dimerization of ethyl sinapate **1** into **8** resulted in a 1.4-fold increase in the maximum absorbance as well as a better wavelength range coverage (ethyl sinapate **1**: 260–370 nm and  $\beta$ - $\beta'$  ethyl sinapate dimer **8**: 260–402 nm), enabling dimer **8** to absorb both in the UV-A (315–400 nm) and the UV-B (280–315 nm) regions. With regard to the nature of the ester moiety, the data obtained for compounds **8**–**14** showed a similar wavelength coverage, except for **13** that exhibits a bathochromic shift (Fig. 3A and B). Only a significant difference in the absorbance levels could be observed, with a factor of 1.2 between the highest (**9**) and the lowest (**10**). In conclusion, the extended conjugation brought about by the dimerization did increase the wavelength range and result in the maximum absorbance. All synthesized dimers (**8**–**14**) proved to have a higher absorbance value and a wider wavelength coverage than both reference molecules (Fig. 3A and B), thus showing that  $\beta$ - $\beta'$  sinapate ester dimers are potent bio-based anti-UV compounds, able to simultaneously cover the UV-A and the UV-B regions.

Dean *et al.*<sup>6</sup> demonstrated that the conjugation and the ester moieties in sinapate derivatives played an important role in their UV properties. This observation was confirmed by comparing  $\beta$ - $\beta'$  ethyl sinapate **8** with **17** and **18** (Fig. 4). Indeed, the loss of conjugation resulting from the reduction of the carbon–carbon double bonds led to a severe decrease of the UV properties, **17** only covering from 260 to 290 nm with little absorbance. Reduction of the ester moieties into the



**Scheme 5** Structure of Octinoxate™ (left) and sinapoyl malate (right).

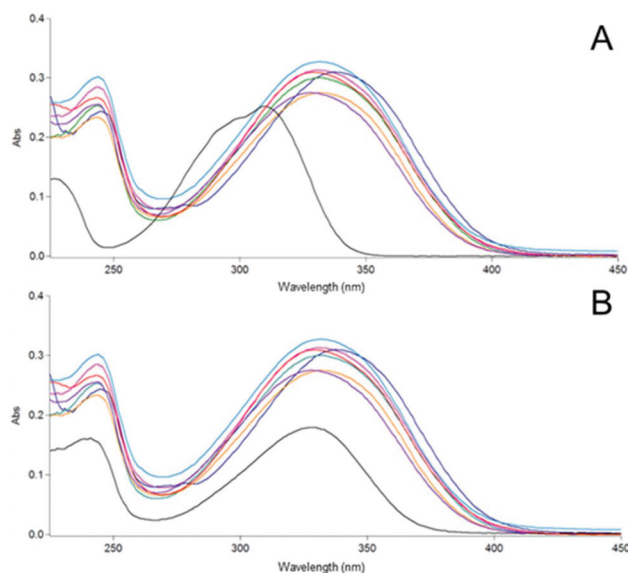


**Fig. 3** UV spectra ( $C = 1 \times 10^{-5}$  mol L<sup>-1</sup> in ethanol) of commercial Octinoxate™ (A) and sinapoyl malate (B) compared to  $\beta$ - $\beta'$  dimers **8** (pink), **9** (light blue), **10** (orange), **11** (purple), **12** (green), **13** (blue) and **14** (red).

corresponding alcohols **18** led to a less severe decrease of absorbance (by a factor of 1.5) covering from 260 to 320 nm. The impact of the free phenol was then investigated by comparing the absorbance of **8** with that of **15** and **16**. Only a slight decrease of the absorbance could be noticed for the two molecules, with a hypsochromic shift, showing that the wavelength coverage could be modulated *via* functionalization of the phenol moiety.

### Antiradical properties

The capacity of  $\beta$ - $\beta'$  sinapate ester dimers (**8–14** and **17** and **18**) to scavenge radicals was assessed. The antiradical activity of the molecules was expressed *via* the EC<sub>50</sub> (half maximal effective concentration) value, defined as the quantity (in nmol) of the antiradical molecule needed to scavenge 50% of the initial quantity of free radicals in the solution. The lower the EC<sub>50</sub>, the higher the antiradical activity. We first performed the DPPH analysis (2,2-diphenyl-1-picrylhydrazyl (DPPH')) rou-

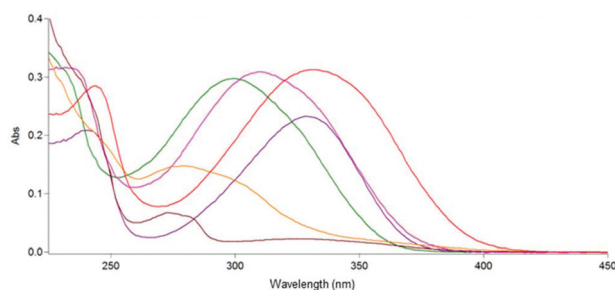
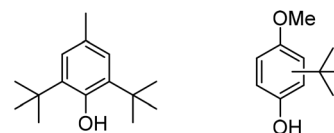


**Fig. 4** UV spectra ( $C = 1 \times 10^{-5}$  mol L<sup>-1</sup>) for SARs between **1** (purple), **8** (red), **15** (pink), **16** (green), **17** (brown) and **18** (orange).

tinely employed in our lab. Unfortunately, its reaction with the  $\beta$ - $\beta'$  sinapate ester dimers led to the apparition of a new band of absorbance at 520 nm, the very same wavelength used to monitor the disappearance of DPPH'. To overcome this issue, another procedure – adapted from Re *et al.*<sup>24</sup> – involving the monitoring of the decrease of the ABTS<sup>•+</sup> radical cation (2,2'-azino-bis(3-ethylbenzothiazoline-6-sulfonic acid)) at 734 nm was performed in duplicate. To assess the potential of our molecules as antiradical compounds, the  $\beta$ - $\beta'$  sinapate ester dimers (**8–14**) and their reduced counterparts (**17** and **18**) were benchmarked against two commercial antioxidants used in food, cosmetics and plastic industries, BHT (butylated hydroxytoluene) and BHA (butylated hydroxyanisole) (Scheme 6).

The data reported in Fig. 5 show a narrow range of EC<sub>50</sub> values (3.52–6.51 nmol) for the  $\beta$ - $\beta'$  sinapate ester dimers (**8–14**). Overall, the nature of the ester moiety did not significantly impact the antiradical activity (4.97–6.51 nmol, Fig. 5), except for dimer (**14**) that had an EC<sub>50</sub> value of 3.52 nmol – most probably due to the higher steric hindrance of the malate moieties.<sup>8</sup> The reduction of conjugation on (**17**) and (**18**) also led to lower EC<sub>50</sub> values, 3.63 nmol and 2.73 nmol, respectively. Such an improvement of the antiradical activity due to the reduction of the carbon-carbon double bond (**17**) has already been described by Reano *et al.*<sup>36</sup> on *p*-hydroxycinnamic bis- and trisphenols.

To assess the impact of the extended conjugation brought about by the dimerization, one should compare the EC<sub>50</sub> of a given dimer to half that of its corresponding monomer (gain =  $1 - [\text{EC}_{50}(\text{dimer})/(\text{EC}_{50}(\text{monomer})/2)]$ ); if the gain was greater than zero, then the impact of the extended conjugation was positive, and the other way around. From Fig. S4 in the ESI† and Table 4, it can be seen that dimerization slightly increased the antiradical activity only in the case of esters bearing the large groups (*i.e.*, 2-ethylhexyl (**10**), *t*-Bu (**11**) and di-*t*-butylmalate (**14**)) and for dialcohol (**18**).



**Scheme 6** Structure of BHT (left) and BHA (right).

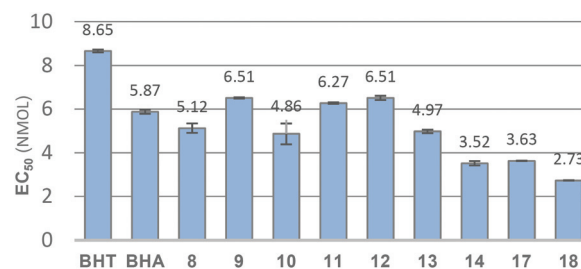


**Fig. 5** Antiradical properties determined by the ABTS<sup>•+</sup> assay: benchmarking of the sinapate ester  $\beta$ - $\beta'$  dimers (**8–18**) against BHT and BHA.

**Table 4** Impact of the  $\beta$ - $\beta'$  dimerization on the antiradical properties

$\beta$ - $\beta'$ dimers	Gain
8	-0.52
9	-0.05
10	0.11
11	0.07
12	-0.19
13	-0.11
14	0.24
17	-0.13
18	0.03

Finally, when compared to the benchmarks, all synthesized  $\beta$ - $\beta'$  dimers exhibited better antiradical activity than BHT; however, only (8), (10), (13), (14), (17) and (18) showed higher activity than BHA. These data undoubtedly demonstrate that  $\beta$ - $\beta'$  sinapate ester dimers are promising bio-based antiradical compounds.

## Conclusions

A sustainable and highly selective biomimetic  $\beta$ - $\beta'$  dimerization of sinapate esters, involving copper as the catalyst, pyridine as the ligand, air as the oxidizing agent and Cyrene™ as the renewable solvent, has been successfully optimized and validated on the multigram scale. The use of the green solvent Cyrene™ allowed reducing the quantity of pyridine used drastically, while improving the yield of the dimerization and reducing the reaction time. The constitution of a library of various  $\beta$ - $\beta'$  sinapate ester dimers and derivatives, and the study of their anti-UV capacity and their antiradical activity through UV analysis and ABTS<sup>+</sup> assays, respectively, allowed the determination of SARs. The results showed that  $\beta$ - $\beta'$  sinapate ester dimers not only covered all the UV-A and UV-B regions, but also exhibited free radical scavenging activity. Finally, benchmarking against recognized anti-UV ingredients and antioxidants showed that the  $\beta$ - $\beta'$  sinapate esters dimers had a great potential as bio-based UV filters and antiradical compounds. The use of these symmetric dimers as monomers for the production of renewable aromatic polyesters, polycarbonates and epoxy resins will be reported in due course.

## Conflicts of interest

F. A., A. L. F. and M. M. M. have filed a patent based on the work described here (patent application no. FR1859902).

## Acknowledgements

The authors are grateful to the Circa Group for providing them with industrial grade Cyrene™. This project was funded by the Agence Nationale de la Recherche under the grant ANR-17-CE07-0046, the EU's Horizon 2020 programme under the grant

no. 828753, Région Grand Est, Conseil Départemental de la Marne and Grand Reims.

## Notes and references

- N. Niciforovic and H. Abramovic, *Compr. Rev. Food Sci. Food Saf.*, 2014, **13**, 34–51.
- H. Nowak, K. Kujawa, R. Zadernowski, B. Rocznik and H. Kozłowska, *Fett Wiss. Technol.*, 1992, **94**, 149–152.
- K.-J. Yun, D.-J. Koh, S.-H. Kim, S. J. Park, J. H. Ryu, D.-G. Kim, J.-Y. Lee and K.-T. Lee, *J. Agric. Food Chem.*, 2008, **56**, 10265–10272.
- E. A. Hudson, P. A. Dinh, T. Kokubun, M. S. J. Simmonds and A. Gescher, *Cancer Epidemiol., Biomarkers Prev.*, 2000, **9**, 1163–1170.
- B. H. Yoon, J. W. Jung, J.-J. Lee, Y.-W. Cho, C.-G. Jang, C. Jin, T. H. Oh and J. H. Ryu, *Life Sci.*, 2007, **81**, 234–240.
- J. C. Dean, R. Kusaka, P. S. Walsh, F. Allais and T. S. Zwieter, *J. Am. Chem. Soc.*, 2014, **136**, 14780–14795.
- M. D. Horbury, E. L. Holt, L. M. M. Mouterde, P. Balaguer, J. Cebrian, L. Blasco, F. Allais and V. G. Stavros, *Nat. Commun.*, 2019, **10**, 1–8.
- L. A. Baker, M. D. Horbury, S. E. Greenough, F. Allais, P. S. Walsh, S. Habershon and V. G. Stavros, *J. Phys. Chem. Lett.*, 2016, **7**, 56–61.
- R. Das, C. Bhattacharjee and S. Ghosh, *Ind. Eng. Chem. Res.*, 2009, **48**, 4939–4947.
- K. Lacki and Z. Duvnjak, *Appl. Microbiol. Biotechnol.*, 1996, **45**, 530–537.
- A. Thiel, K. Muffler, N. Tippkoetter, K. Suck, U. Sohling, S. M. Hruschka and R. Ulber, *J. Chem. Technol. Biotechnol.*, 2015, **90**, 1999–2006.
- M. Janvier, L. Hollande, A. S. Jaufurally, M. Pernes, R. Menard, M. Grimaldi, J. Beaugrand, P. Balaguer, P.-H. Ducrot and F. Allais, *ChemSusChem*, 2017, **10**, 738–746.
- C. Peyrot, A. A. M. Peru, L. M. M. Mouterde and F. Allais, *ACS Sustainable Chem. Eng.*, 2019, **7**, 9422–9427.
- C. S. Lancefield and N. J. Westwood, *Green Chem.*, 2015, **17**, 4980–4990.
- J. van Schijndel, L. A. Canalle, J. Smid and J. Meuldijk, *Open J. Phys. Chem.*, 2016, **6**, 101–108.
- L. M. M. Mouterde and F. Allais, *Front. Chem.*, 2018, **6**, 426.
- G. Wu, M. Heitz and E. Chornet, *Ind. Eng. Chem. Res.*, 1994, **33**, 718–723.
- K. Koschorreck, S. M. Richter, A. B. Ene, E. Roduner, R. D. Schmid and V. B. Urlacher, *Appl. Microbiol. Biotechnol.*, 2008, **79**, 217–224.
- M. Bunzel, J. Ralph, H. Kim, F. Lu, S. A. Ralph, J. M. Marita, R. D. Hatfield and H. Steinhart, *J. Agric. Food Chem.*, 2003, **51**, 1427–1434.
- A. Neudorffer, D. Bonnefont-Rousselot, A. Legrand, M.-B. Fleury and M. Largeton, *J. Agric. Food Chem.*, 2004, **52**, 2084–2091.



- 21 B. Sathish Kumar, A. Singh, A. Kumar, J. Singh, M. Hasanain, A. Singh, N. Masood, D. K. Yadav, R. Konwar, K. Mitra, J. Sarkar, S. Luqman, A. Pal, F. Khan, D. Chanda and A. S. Negi, *Bioorg. Med. Chem.*, 2014, **22**, 1342–1354.
- 22 F. Lu and J. Ralph, *Org. Biomol. Chem.*, 2008, **6**, 3681–3694.
- 23 W. Li, H. Liu, J. Xu, P. Zang, Q. Liu and W. Li, *Eur. J. Org. Chem.*, 2014, 3475–3482.
- 24 R. Re, N. Pellegrini, A. Proteggente, A. Pannala, M. Yang and C. Rice-Evans, *Free Radical Biol. Med.*, 1999, **26**, 1231–1237.
- 25 A. S. Jaufurally, A. R. S. Teixeira, L. Hollande, F. Allais and P.-H. Ducrot, *ChemistrySelect*, 2016, **1**, 5165–5171.
- 26 F. Yue, F. Lu, R. Sun and J. Ralph, *Chem. – Eur. J.*, 2012, **18**, 16402–16410.
- 27 T. Kobayashi, H. Taguchi, M. Shigematsu and M. Tanahashi, *J. Wood Sci.*, 2005, **51**, 607–614.
- 28 U. Takahama, *Physiol. Plant.*, 1995, **93**, 61–68.
- 29 S. Riva, *Trends Biotechnol.*, 2006, **24**, 219–226.
- 30 J. C. J. M. D. S. Menezes, S. P. Kamat, J. A. S. Cavaleiro, A. Gaspar, J. Garrido and F. Borges, *Eur. J. Med. Chem.*, 2011, **46**, 773–777.
- 31 J. Padwal, W. Lewis and C. J. Moody, *Org. Biomol. Chem.*, 2011, **9**, 3484–3493.
- 32 F. Allais, S. Martinet and P.-H. Ducrot, *Synthesis*, 2009, 3571–3578, DOI: 10.1055/s-0029-1216983.
- 33 J. Sherwood, M. De Bruyn, A. Constantinou, L. Moity, C. R. McElroy, T. J. Farmer, T. Duncan, W. Raverty, A. J. Hunt and J. H. Clark, *Chem. Commun.*, 2014, **50**, 9650–9652.
- 34 A. A. C. Pacheco, J. Sherwood, A. Zhenova, C. R. McElroy, A. J. Hunt, H. L. Parker, T. J. Farmer, A. Constantinou, M. De Bruyn, A. C. Whitwood, W. Raverty and J. H. Clark, *ChemSusChem*, 2016, **9**, 3503–3512.
- 35 L. M. M. Mouterde, F. Allais and J. D. Stewart, *Green Chem.*, 2018, **20**, 5528–5532.
- 36 A. F. Reano, J. Cherubin, A. M. M. Peru, Q. Wang, T. Clement, S. Domenek and F. Allais, *ACS Sustainable Chem. Eng.*, 2015, **3**, 3486–3496.